A 3D Finite Element Analysis of Bone Tissue in 3-Unit Implant-Supported Prostheses: Effect of Splinting Factor and Implant Length and Diameter

Keywords

Dental Implant
Finite Element Analysis
Dental Prosthesis

Authors

Victor E. de Souza Batista *
(DDS, MSc, PhD)

Fellippo R. Verri §
(DDS, MSc, PhD)

Cleidiel A. Lemos ‡
(DDS, MSc, PhD)

Ronaldo S. Cruz Δ
(DDS, MSc, PhD)

Pedro Y. Noritomi ^
(Eng, MSc, PhD)

Eduardo P. Pellizzer †
(DDS, MSc, PhD)

Address for Correspondence

Victor E. de Souza Batista *

Email: victor_edsb@hotmail.com

* *Associate Professor, Department Prosthodontics, Presidente Prudente Dental School, University of Western São Paulo - UNOESTE, José Bongiovani St, 700, Presidente Prudente, São Paulo 19050-920, Brazil*

§ *Adjunct Professor, Department of Dental Materials and Prosthodontics, Araçatuba Dental School (UNESP), Univ Estadual Paulista, Araçatuba, Brazil*

‡ *Adjunct Professor. Department of Dentistry (Division of Prosthodontics), Federal University of Juiz de Fora, Campus Avançado Governador Valadares (UFJF/GV), Governador Valadares, Minas Gerais, Brazil*

Δ *Department of Dental Materials and Prosthodontics, Araçatuba Dental School (UNESP), Univ Estadual Paulista, Araçatuba, Brazil*

^ *Researcher, Information Tecnology Center Renato Archer, Campinas, SP, Brazil*

† *Titular Professor, Department of Dental Materials and Prosthodontics, Araçatuba Dental School (UNESP), Univ Estadual Paulista, Araçatuba, Brazil*

Received: 06.05.2020
Accepted: 07.09.2020

doi: 10.1922/EJPRD_2098deSouzaBatista08

ABSTRACT

This study aimed to assess the effects of splinting in 3-unit implant-supported prostheses with varying the splinting factor, length of the implant, and the diameter of the 1ºmolar (1ºM) implant on cortical bone tissue (CBT). Twelve 3D models were simulated, which represented the posterior maxillary with 3 implants, supporting 3-unit FDP varying the splinting factor (single-unit crowns, splinted crowns straight-line and offset implant configuration [OIC]), length of the implant (7mm and 8,5mm), and the diameter of the 1ºM (Ø4 mm and Ø5 mm). The CBT was analyzed by maximum principal stress and microstrain maps. The increase in implant diameter improved the biomechanical behavior of rehabilitation. The increase of the implant diameter in the 1ºM associated with OIC generated the best biomechanical behavior for CBT. The splinting was effective in decreasing stress and microstrain, mainly when associated with OIC and implant diameter of Ø5 in the 1ºM. The effect of increasing the diameter of the implant referring to the 1ºM for single-unit crowns was more effective than the effect of the splinting of implants with Ø4 mm in straight-line. The diameter and splinting factors showed to be more important than implant length to reduce the stress and microstrain on CBT.

INTRODUCTION

The rehabilitation of patients with partial edentulism – such as in Kennedy class I and II scenarios – in the posterior maxilla (scenarios with missing premolars and a molar, or a missing second premolar and 2 molars) with dental implants is a challenge, since the literature has associated a greater tendency to implant failure in this region because it is an area of lower bone density that receives a greater occlusal force (Misch, 1999; Goiato *et al.*, 2014).

The reduced height of the bone crest of this area has been usually associated with the pneumatization of the maxillary sinus (Perelli *et al.*, 2012) and, sometimes, it is not possible the placement of longer dental implants (LDIs), but it allows the placement of an dental implant with a larger diameter (Mendonça *et al.*, 2014). This way, the placement of short dental implants (SDI) (<10mm) has been suggested in order to avoiding invasive surgical procedures, reduces the morbidity, time and cost of the rehabilitative treatment (Perelli *et al*., 2012). However, the success of the planning using SDI is controversial (Mendonça *et al*., 2014). Lemos *et al*. 2016 published a systematic review and meta-analysis comparing SDI (< 8mm) with standard length implants and they concluded that dental implants with a length of less than 8mm (4 to 7mm) should be used with caution, since they have a large risk of dental implant failures when compared to standard length implants; however, the splinting factor was not considered in the systematic review (Lemos *et al*., 2016).

In this context, the splinting of the dental implant may favor the load sharing between the dental implants and dissipate the stress more favorably to the bone tissue, avoiding the overload, especially when the dental implants were positioned in poor bone quality (de Souza Batista *et al*., 2017a; Mendonça *et al*., 2014) or when the association of SDI with a LDI was planned (Pellizzer *et al*., 2014; Pellizzer *et al*., 2015). Nonetheless, more attention to obtain passivity of the restoration as well as better instruction and training in order to maintain an adequate oral hygiene are necessary for patients who use splinted prostheses (Solnit & Schneider 1998; Vázquez Álvarez *et al*., 2015). Faced with these facts, the clinical indecision between splinting or not the prosthesis is still common among professionals that it has been acted in the area of implantology (Mendonça *et al*., 2014).

In the context of the splinting, a modification in the placement of the central implant (for vestibular or lingual) – configuring the tripoidal positioning – has been suggested as an alternative for straight-line implants supporting 3-unit splinted fixed dental prosthesis (FDP). A 3-dimentional (3D) finite element analysis (FEA) study showed the biomechanical advantages in using the offset implant configuration to rehabilitate the posterior maxilla; however, only external implants with 10 mm of length was studied (de Souza Batista *et al*. 2017a). Furthermore, the effect of the offset implant configuration is still not fully understood (Batista *et al*., 2015), mainly in its relation to biomechanical behavior in SDIs or SDIs associated with a LDI with different diameter.

The diameter of the dental implant is another important factor to be assessed, since the literature has reported that larger diameter implants have generated an improvement in the biomechanical behavior of the rehabilitation (Santiago Junior *et al*., 2016; Minatel *et al*., 2017; Meimandi *et al*., 2018). Previous biomechanical studies showed that dental implants of Ø4 mm x 10 mm placed in the molar area tend to receive greater masticatory forces, especially when the FDP was not splinted (de Souza Batista *et al*., 2017a; Lemos *et al*., 2018). Thus, in the context of planning the placement of three dental implants to support the replacement of missing premolars and a molar, would the increase of the diameter of the dental implant in the molar area avoid the use of splinted crowns? The data needed to answer this question are scarce in the literature.

The 3D-FEA is a useful tool to better understand the biomechanical behavior in the association of these factors (splinting, length and implant diameter) and the data offered after analysis may contribute to improve the surgical and prosthetic planning (Pirmoradian *et al*. 2019).

The purpose of this 3-dimensional (3D) finite element analysis was to assess the effects of splinting in 3-unit implant-supported prostheses with varying the splinting factor (single-unit crowns, splinted crowns straight-line and offset implant configuration), length of the dental implant (7mm and 8,5mm), and the diameter of the 1ºmolar implant (Ø4 mm e Ø5 mm). The null hypothesis was that the studied variables would not generate differences in the biomechanical behavior of the bone tissue.

MATERIAL AND METHODS

EXPERIMENTAL DESIGN

The methodology used followed previously published studies (Santiago Junior *et al*., 2016; Minatel *et al*., 2017; de Souza Batista *et al*., 2017b; Lemos *et al*., 2018). This research was developed considering the following factors: splinting (single-unit crowns, splinted crowns with straight-line implants and offset implant configuration), length of the implant of the 2ºPM and 1ºM (7mm and 8,5mm), and the increase of diameter of the 1ºmolar implant (Ø4 mm e Ø5 mm), under axial and oblique loading.

3D MODELING

Twelve 3D models were simulated to represent clinical situations *(Table 1)*. The models represented the posterior maxillary segment (first premolar to first molar) with three external hexagon (HE) implants (Conexão Sistemas de Prótese Ltda., Arujá, São Paulo, Brasil) supporting 3-unit FDP, screw retained.

The modeling of the bone tissue followed previously published studies (de Souza Batista *et al*. 2017a). For this stage, the in Vesalius software (CTI Renato Archer) was used to obtain the stereolithography file, then the surface simplification was performed in the program Rhinoceros 4.0 (NURBS Modeling for Windows, Seattle, Washington, EUA).

The dental implant design was obtained by simplification of an external hexagonal design (Verri *et al*., 2016). The distance of the dental implants was the same for all simulated models as preconized in previously published studies (de Souza Batista *et al*., 2017a). The intermediate dental implant – relative to the second premolar – was horizontally displaced by 1.5 mm in the buccal direction in the offset implant configuration models (de Souza Batista *et al*., 2018). Single-unit and splinted FDP was simulated in straight-line. Screw-retained metal-ceramic restoration was simulated for all models.

Table 1. Description of models.

Models	Type of Prosthesis/ Implant Position	Diameter/Length			No. of Nodes/ Elements
		1º PM	2º PM	1º M	
M1	Single-unit crowns/ straight-line	Ø4 mm x 10 mm	Ø4 mm x 8,5 mm	Ø4 mm x 8,5 mm	833.345/ 1.764.983
M2	Splinted crowns/ straight-line	Ø4 mm x 10 mm	Ø4 mm x 8,5 mm	Ø4 mm x 8,5 mm	773.212/ 1.669.827
M3	Splinted crowns/ offset	Ø4 mm x 10 mm	Ø4 mm x 8,5 mm	Ø4 mm x 8,5 mm	741.266/ 1.623.719
M4	Single-unit crowns/ straight-line	Ø4 mm x 10 mm	Ø4 mm x 7 mm	Ø4 mm x 7 mm	819.762/ 1.743.659
M5	Splinted crowns/ straight-line	Ø4 mm x 10 mm	Ø4 mm x 7 mm	Ø4 mm x 7 mm	754.523/ 1.640.937
M6	Splinted crowns/ offset	Ø4 mm x 10 mm	Ø4 mm x 7 mm	Ø4 mm x 7 mm	682.310/ 1.532.596
M7	Single-unit crowns/ straight-line	Ø4 mm x 10 mm	Ø4 mm x 8,5 mm	Ø5 mm x 8,5 mm	751.679/ 1.639.990
M8	Splinted crowns/ straight-line	Ø4 mm x 10 mm	Ø4 mm x 8,5 mm	Ø5 mm x 8,5 mm	749.623/ 1.635.632
M9	Splinted crowns/ offset	Ø4 mm x 10 mm	Ø4 mm x 8,5 mm	Ø5 mm x 8,5 mm	702.381/ 1.562.564
M10	Single-unit crowns/straight-line	Ø4 mm x 10 mm	Ø4 mm x 7 mm	Ø5 mm x 7 mm	724.914/ 1.597.072
M11	Splinted crowns/ straight-line	Ø4 mm x 10 mm	Ø4 mm x 7 mm	Ø5 mm x 7 mm	722.440/ 1.590.232
M12	Splinted crowns/ offset	Ø4 mm x 10 mm	Ø4 mm x 7 mm	Ø5 mm x 7 mm	724.928/ 1.595.476

1º PM, first premolar; 2º PM, second premolar; 1º M, first molar; Ø, diameter; mm, millimeter.

Dental implants, abutments, crowns, and abutment screws were simplified using SolidWorks (SolidWorks Corp) and Rhinoceros software (NURBS modeling for Windows [Microsoft Corp]; Robert McNeel & Associates). Subsequently, all geometries were exported to discretization in the FEMAP software 11.4.2 (Siemens PLM Software Inc).

CONFIGURATION OF THREE-DIMENSIONAL ANALYSIS AND INTERFACES CONDITIONS, BOUNDARY AND LOADS

Meshes with tetrahedral parabolic solid elements were generated in the preprocessing stage in the FEMAP 11.4.2 software. In this stage, the mechanical properties of each simulated material used in the 3D model were attributed to the meshes (Sertgöz, 1997; Sevimay *et al.*, 2005; Verri *et al.*, 2017) *(Table 2)*. All materials were considered linearly elastic, homogeneous, and isotropic. The abutment/dental implant contact was configured as symmetrical, and all other contacts were configured as symmetrically welded. The boundary conditions were established as fixed in all axes in the upper surface of the bone block (de Souza Batista *et al.*, 2017a). The applied forces were 400 N axially – 50 N at each cusp tip – and 200 N obliquely – 50 N applied at 45° in each lingual cusp ridge of buccal cusp.

Table 2. Mechanical properties applied in finite element analysis

Structure	Elastic Modulus (GPa)	Poisson ratio (v)	Reference
Trabecular bone with low density (type IV bone)	1.10	0.30	Sevimay et al., 2005
Cortical bone	13.7	0.30	Sertgöz et al., 1997
Titanium (abutment screw and dental implant)	110.0	0.35	Sertgöz et al., 1997
Ni-Cr alloy	206.0	0.33	Verri et al. 2017
Feldspathic porcelain	82.8	0.35	Verri et al. 2017

GPa, gigapascal; NiCr, Nickel-Chromium

FINITE ELEMENT ANALYSIS

All mathematical problems were processed by Nei Nastran 11.1 (Noran Engineering, Inc., Westminster, California, USA) to obtain the results. After data processing, the results were exported to FEMAP 11.4.2 for graphical visualization of stress and strain (Santiago Junior *et al.*, 2016; Minatel *et al.*, 2017; de Souza Batista *et al.*, 2017b) in the bone tissue by using of maps of maximum principal stress and microstrain (με – strain x10^{-6}). The maximum principal stress may offer values of compressive (negative values) and tractive (positive values) stress (Torcato *et al.*, 2014; Verri *et al.*, 2014; Santiago Junior *et al.*, 2016; de Souza Batista *et al.*, 2017b). The microstrain was used to obtain values to compare with the scale of risk of resorption provided by Frost (Frost, 2003). The unit of measurement for the maximum principal stress was MegaPascal (MPa). The με was measured by the strain unit x10-6, and its magnitude is dimensionless.

RESULTS

MAXIMUM PRINCIPAL STRESS ANALYSIS

Low values of tensile stress and compression in the cortical bone tissue around the dental implants were visualized in axial loading for all simulated models (*Figure 1*). In general, the highest values of tensile and compressive stress were visualized in the oblique loading when compared to the axial loading (*Figure 2*).

Using scale of -10MPa to 40MPa, the oblique loading generated a greater area of tensile stress in the palatal region of the cortical bone tissue around the dental implants. A greater area of tensile stress (range of 30,6 MPa – 40 MPa) was visualized in the palatal region of the cortical bone tissue around the 1ºM implant of the M1 and M4 models when compared to the other models. However, the increase in implant diameter in the 1ºM implant region caused the reduction of this tensile stress area (M7 and M10). The M2, M5, M8 and M11 models showed a reduction of the tensile stress area in the palatal region (range of 18,13MPa to 40MPa) of the bone tissue around the 1ºM implant when compared to the M1, M4, M7 and M10 models, respectively, but they showed an increase of the area of tensile stress in the bone tissue around the 1ºPM and 2ºPM. Still in this context, the increase of the implant diameter in the region of the 1ºM (M8 and M11) favored the biomechanical behavior of the splinted crown with straight-line implants. Furthermore, the models with offset implant configuration (M3, M6, M9 e M12) reduced the area of tensile stress in the palatal region of the cortical bone tissue around the 2ºPM implant when compared to single-unit crowns and splinted crowns with straight-line implants models (M2, M5, M8 and M11, respectively). In general, the

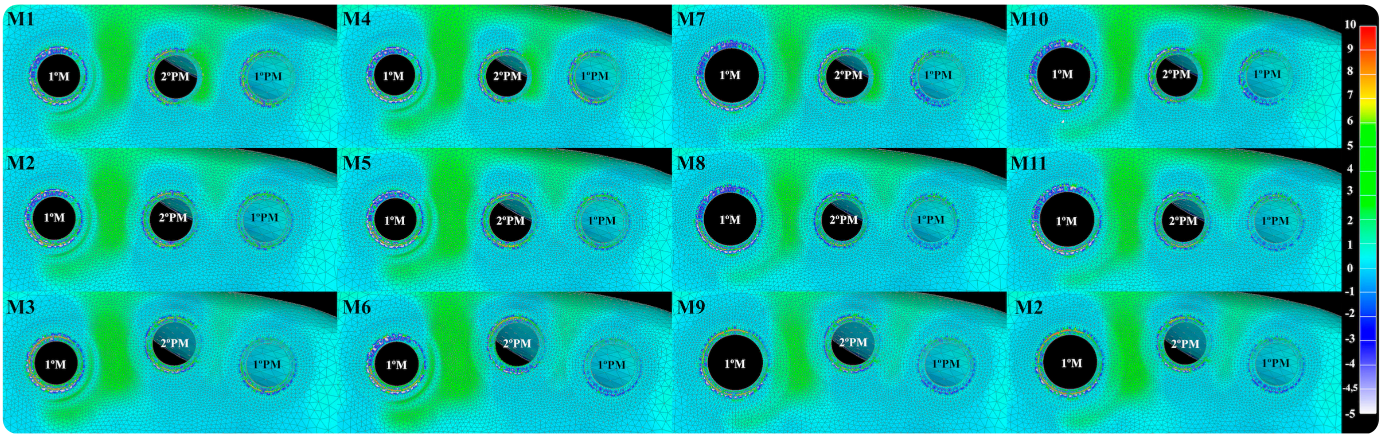

Figure 1: Maximum principal stress on cortical bone tissue, axial loading, occlusal view.

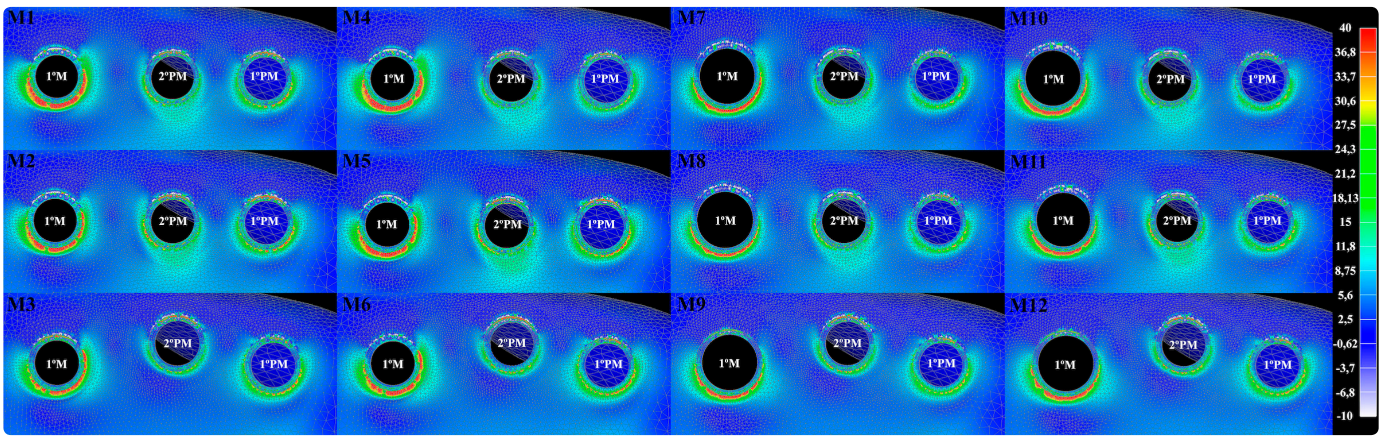

Figure 2: Maximum principal stress on cortical bone tissue, oblique loading, occlusal view.

increase of the diameter of the dental implants in the 1°M region was efficient to improve the biomechanical behavior of the rehabilitation, especially for dental implants with single-unit crowns (M7 and M10) that presented biomechanical behavior similar to the M2 and M5 models. Conversely, the reduction of the dental implants lengths of the 2°PM and 1°M of 8.5 mm to 7.0 mm resulted in the increase of tensile stress in the bone tissue around the 1°M.

MICROSTRAIN ANALYSIS

Low values of microstrain in the cortical bone tissue around the dental implants were visualized in axial loading for all simulated models (*Figure 3*). In general, the highest values of microstrain were visualized in the oblique loading when compared to the axial loading (*Figure 4*).

The oblique loading generated a larger area of microstrain in the vestibular region of the cortical bone around the dental implants for all the models. The M1 and M4 models presented a larger area of microstrain (range of 5,200 με to 6,000 με) in the vestibular region of the cortical bone tissue around the 1°M implant when compared to the other models; however, the increase in implant diameter in the 1°M region caused the reduction of the microstrain in this area (M7 and M10). The M2 and M5 models presented a reduced area of microstrain in the bone tissue around the 1°M when compared to the M1 and M4 models, respectively, but this difference was not clearly observed between M7 (against M8) and M10 (against M11). The M3, M6, M9 and M12 models decreased the area of microstrain in the bone tissue around the 1°PM and 1°M when compared with the M2, M5, M8 and M11 models, respectively, but they showed an increase in the microstrain area in the bone tissue around the 2°PM. The increase in implant diameter in the 1°M region associated to offset implant configuration (M9 and M12) generated the best biomechanical behavior, mainly to reduce the area of microstrain in the vestibular region of the 1°M, in special for single-unit crowns (M7 and M10) that showed a reduction in the value of microstrain when compared to M2 and M5 models (*Figure 5*).

In general, the reduction of the implant length of the 2° PM and 1°M of 8.5 mm to 7.0 mm generated an increase of microstrain in the bone tissue around the dental implants.

DISCUSSION

The null hypothesis of the present study was rejected since the studied variables – splinting, length of the dental implant of the 2°PM and 1°M, and the increase of diameter of the 1°molar implant – generated different patterns of stress/strain distribution in the bone tissue.

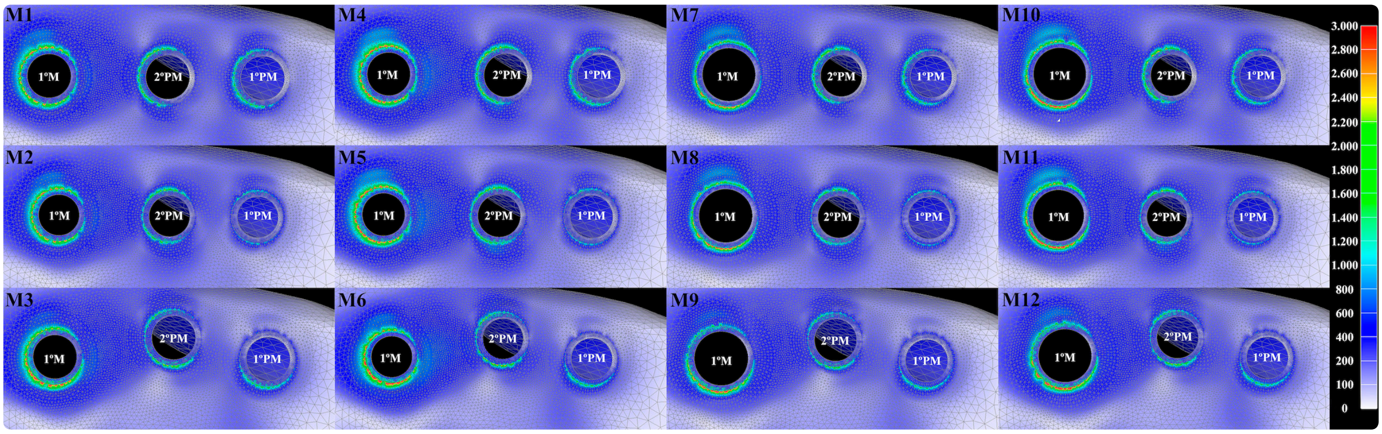

Figure 3: Microstrain on cortical bone tissue, axial loading, occlusal view.

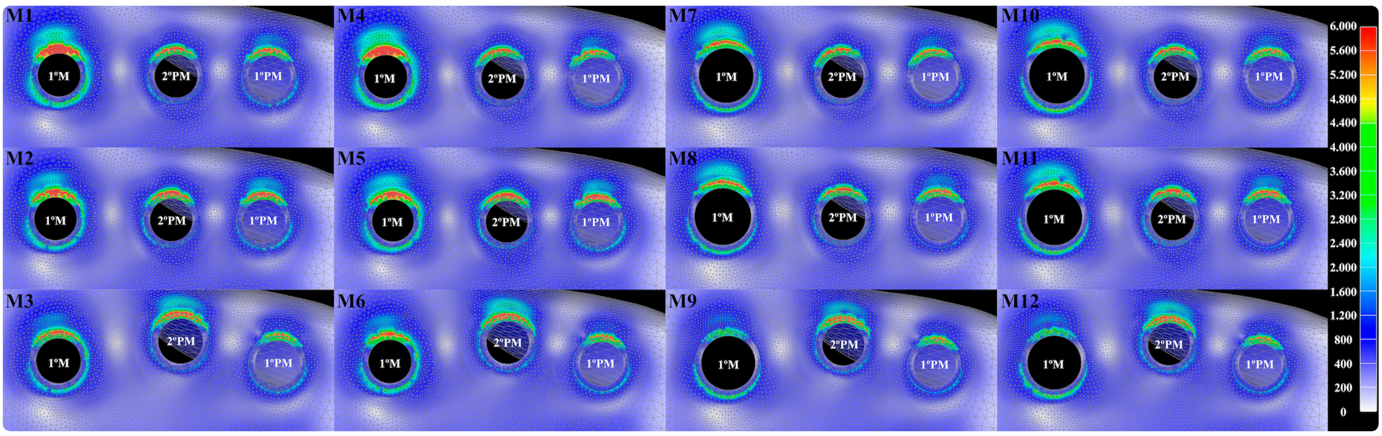

Figure 4: Microstrain on cortical bone tissue, oblique loading, occlusal view.

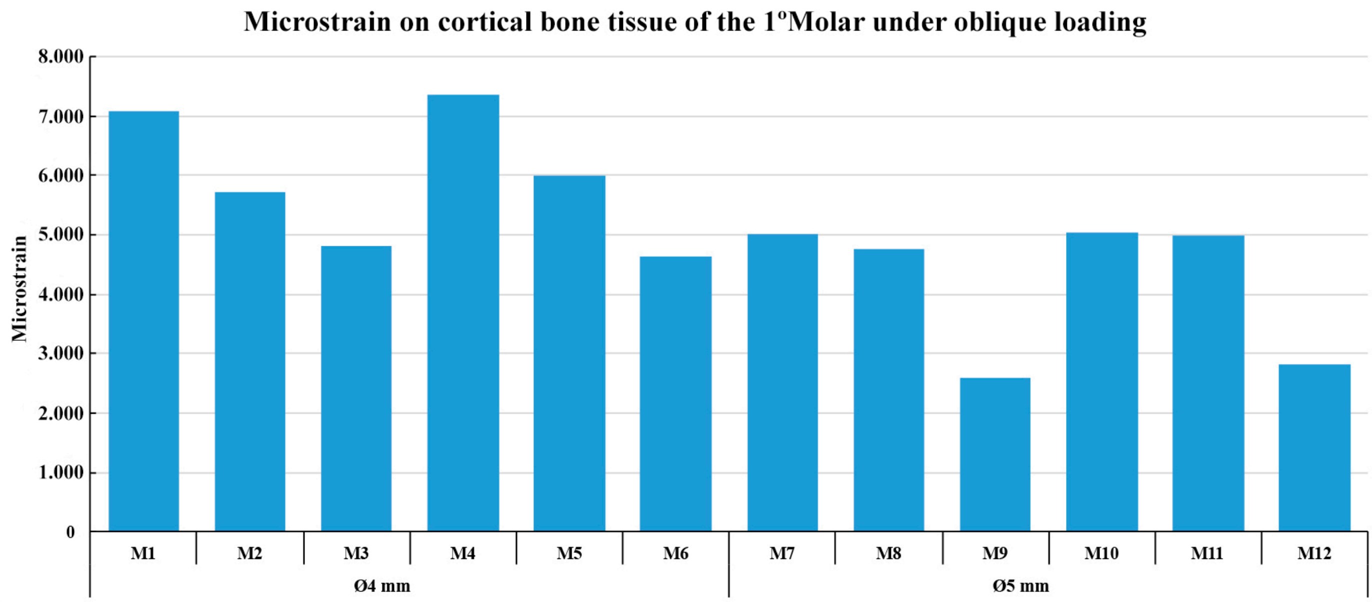

Figure 5: Microstrain values on cortical bone under oblique loading.

The oblique loading increased the stress and strain values on cortical bone when compared to axial loading for all simulated models. This result is in accordance with previous published studies using FEA (de Souza Batista *et al*., 2017a; Lemos *et al*., 2018; Meimandi *et al*., 2018). Area of tensile/tractive stress in the palatal region and compressive stress in the vestibular region of the cortical bone tissue around the dental implants occurred due to the direction to the load – 50 N applied at 45° in each lingual cusp ridge of buccal cusp – applied in the present study.

In agreement with previous published studies (de Souza Batista *et al*., 2017a; Lemos *et al*., 2018), the results of the present study suggest a biomechanical beneficial of the splinting mainly associated to offset implant configuration. The literature report that the splinting may favor the sharing of stress between dental implants of the rehabilitation, due to the rigid structure acts to join the dental crowns, consequently, decreasing the stress and strain on bone tissue (Pellizzer *et al*., 2015; Lemos *et al*., 2018).

The increase of the implant diameter improved the biomechanical behavior of prosthetic planning. This data agrees with previously published studies that demonstrated this biomechanical benefit for unitary dental implant (Minatel *et al*., 2017) and for multiple dental implants (Akça K & Iplikçioğlu, 2001). This improvement may have occurred by the fact of the dental implants with larger diameter dissipate the occlusal force with more effectiveness due to an increase of its surface area and mass (Akça K & Iplikçioğlu, 2001).

Planning the placement of the dental implant, type of connection, type of prosthesis prior to dental implant placement – reverse planning – is fundamental for success (Block, 2018). Thus, the present study may contribute to a better understanding of the biomechanical behavior of different possibilities of dental implant rehabilitation in the posterior maxilla. In fact, the increase in the diameter of the dental implant in the area of the 1ºM associated with offset implant configuration generated a better biomechanical behavior for the bone tissue. Consequently, to assess the availability of bone tissue is essential using an adequate planning based on clinical and tomographic examination (Block, 2018), mainly for offset implant configuration planning which requires a greater buccal-lingual thickness of bone tissue.

Also, the increase the implant diameter of the 1ºM area (simulated situation in the M7 and M10) predominated on the effect of splinting of dental implants with Ø4 mm in straight-line (simulated situation in the M2 and M5), offering a more favorable biomechanical behavior. Probably, the increase of the contact area between the dental implant and bone tissue – due to the use of large implant diameter – may be more beneficial to decrease the stress and strain on cortical bone than the force sharing provided by the splinting of the crowns. Extrapolating with caution to the clinical routine, the use of single-unit crowns may be viable when the diameter of the dental implant in the molar of Ø5 mm is planned.

The use of dental implants with 7 mm of length caused unfavorable biomechanical behavior when compared to dental implants with 8.5 mm of length, in agreement with a previously published systematic review that observed a greater risk of dental implant failure less or equal to 7 mm (Lemos *et al*., 2016). The literature has reported that the decrease in bone/dental implant contact surface and the unfavorable clinical crown/dental implant ratio may justify this unfavorable biomechanical (Atieh *et al*. 2012; Elangovan *et al*. 2013; Verri *et al*. 2016). Consequently, the use of LDIs – external connection – may be a viable option to improve the biomechanical performance in rehabilitation of three elements in the posterior maxilla.

The materials simulated in the present study were considered isotropic, homogeneous and linearly elastic, as in previous studies (Iplikçioğlu & Akça *et al*., 2002; de Souza Batista *et al*., 2017). However, human tissues – as bone tissue – and dental materials are more dynamic in a clinical scenario in which may generate different results when FEA is compared to data obtained from clinical studies (Iplikçioğlu & Akça *et al*., 2002). Consequently, this factor may be considered a methodological limitation.

Although MEF is an excellent tool for preclinical analysis in implantology area (Pesqueira *et al*., 2014), randomized controlled trials about the effect of the studied variables in the present study on periodontal and bone tissues would provide more accurate data for clinical application in the area of implantology.

CONCLUSION

Within the limitations of the study, it was possible to conclude that:

- the splinting was effective in decreasing stress and microstrain, mainly when associated with offset implant configuration;
- the increase of implant diameter in the 1ºM area was effective to reduce stress and microstrain in the bone tissue;
- biomechanically, the effect of increasing the diameter of the dental implant referring to the 1ºM for single-unit crowns (M7 and M10 situations) was more effective than the effect of the splinting of dental implants with Ø4 mm in straight-line (M2 and M5).
- The diameter and splinting factors showed to be more important than implant length in the reducing stress and microstrain in bone tissue.

DISCLOSURE STATEMENT

No potential conflict of interest was reported by the authors

FUNDING

Supported by grants 2012/24893-1 and 2015/07383-8 from the São Paulo Research Foundation, Brazil.

ACKNOWLEDGMENT

The authors thank Renato Archer Research Center for their supporting in the analysis.

Renato Archer Research Center, Campinas, Sao Paulo, Brazil.

Conexao Sistemas de Protese, Aruja, Sao Paulo, Brazil.

REFERENCES

Atieh, M.A., Zadeh, H., Stanford, C.M., Cooper, L.F. Survival of short dental implants for treatment of posterior partial edentulism: a systematic review. *Int. J. Oral Maxillofac. Implants*. 2012;**27**:1323-1331.

Akça, K., Iplikçioğlu, H. Finite element stress analysis of the influence of staggered versus straight placement of dental implants. *Int. J. Oral Maxillofac. Implants*. 2001;**16**:722-730.

Batista, V.E., Santiago Junior, J.F., Almeida, D.A., Lopes, L.F., Verri, F.R., Pellizzer, E.P. The effect of offset implant configuration on bone stress distribution: a systematic review. *J. Prosthodont*. 2015;**24**:93-99.

Block, M.S. Dental Implants: The Last 100 Years. *J. Oral Maxillofac. Surg*. 2018;**76**:11-26.

de Souza Batista, V.E., Verri, F.R., Almeida, D.A.F., Santiago Junior, J.F., Lemos, C.A.A., Pellizzer, E.P. Evaluation of the effect of an offset implant configuration in the posterior maxilla with external hexagon implant platform: A 3-dimensional finite element analysis. *J. Prosthet. Dent*. 2017a;**118**:363-371.

de Souza Batista, V.E., Verri, F.R., Lemos, C.A.A., Cruz, R.S., Oliveira, H.F.F., Gomes, J.M.L., Pellizzer, E.P. Should the restoration of adjacent implants be splinted or nonsplinted? A systematic review and meta-analysis. *J Prosthet Dent*. 2019;**121**:41-51

de Souza Batista, V.E., Verri, F.R., Almeida, D.A., Santiago Junior, J.F., Lemos, C.A., Pellizzer, E.P. Finite element analysis of implant-supported prosthesis with pontic and cantilever in the posterior maxilla. *Comput. Methods. Biomech. Biomed. Engin*. 2017b;**20**:663-670.

Elangovan, S., Mawardi, H.H., Karimbux, N.Y. Quality assessment of systematic reviews on short dental implants. *J. Periodontol*. 2013;**84**:758-767.

Frost, H.M. Bone's mechanostat: a 2003 update. Anat. Rec. A. Discov. *Mol. Cell Evol. Biol*. 2003;**275**:1081-1101.

Goiato, M.C., dos Santos, D.M., Santiago Jr, J.F., Moreno, A., Pellizzer, E.P. Longevity of dental implants in type IV bone: a systematic review. Int. *J. Oral Maxillofac. Surg*. 2014;**43**:1108-1116.

Iplikçioğlu, H., Akça, K. Comparative evaluation of the effect of diameter, length and number of implants supporting three-unit fixed partial prostheses on stress distribution in the bone. *J. Dent*. 2002;**30**:41-46.

Lekholm, U., Zarb, G. Patient selection and preparation. *Tissue- integrated prostheses: osseointegration in clinical dentistry*. Quintessence Publishing Co, Inc, Chicago, IL. 1985 pp. 199-209.

Lemos, C.A., Ferro-Alves, M.L., Okamoto, R., Mendonça, M.R., Pellizzer, E.P. Short dental implants versus standard dental implants placed in the posterior jaws: A systematic review and meta-analysis. *J. Dent*. 2016;**47**:8-17.

Lemos, C.A.A., Verri, F.R., Santiago, J.F. Jr., Almeida, D.A.F., Batista, V.E.S., Noritomi, P.Y., Pellizzer, D.P. Retention System and Splinting on Morse Taper Implants in the Posterior Maxilla by 3D Finite Element Analysis. *Braz. Dent. J*. 2018;**29**:30-35.

Meimandi, M., Talebi Ardakani, M.R., Amid, R., Mahmoudi Motlagh, A., Beheshti, S. Comparison of Stress and Strain Distribution Around Splinted and Nonsplinted 6-mm Short Implants in Posterior Mandible: A Finite Element Analysis Study. *Implant Dent*. 2018;**27**:74-80.

Mendonça, J.A., Francischone, C.E., Senna, P.M., Matos de Oliveira, A.E., Sotto-Maior, B.S. A retrospective evaluation of the survival rates of splinted and non-splinted short dental implants in posterior partially edentulous jaws. *J. Periodontol*. 2014;**85**:787-794.

Minatel, L., Verri, F.R., Kudo, G.A.H., de Faria Almeida, D.A., de Souza Batista, V.E., Lemos, C.A.A., Pellizzer, E.P., Santiago, J.F. Junior. Effect of different types of prosthetic platforms on stress-distribution in dental implant-supported prostheses. *Mater. Sci. Eng. C. Mater. Biol. Appl*. 2017;**71**:35-42.

Misch, C.E. Implant design considerations for the posterior regions of the mouth. *Implant Dent*. 1999;**8**:376-386.

Nishioka, R.S., de Vasconcellos, L.G., de Melo Nishioka, G.N. Comparative strain gauge analysis of external and internal hexagon, Morse taper, and influence of straight and offset implant configuration. *Implant Dent.* 2011;**20**:e24-32.

Nishioka, R.S., de Vasconcellos, L.G., de Melo Nishioka, L.N. External hexagon and internal hexagon in straight and offset implant placement: strain gauge analysis. *Implant Dent.* 2009;**18**:512-520.

Pellizzer, E.P., de Mello, C.C., Santiago Junior, J.F., de Souza Batista, V.E., de Faria Almeida, D.A., Verri, F.R. Analysis of the biomechanical behavior of short implants: The photo-elasticity method. *Mater Sci. Eng. C. Mater. Biol. Appl.* 2015;**55**:187-192.

Pellizzer, E.P., Santiago Junior, J.F., Ribeiro Villa, L.M., de Souza Batista, V.E., Mello, C.C., de Faria Almeida, D.A., Honório, H.M. Photoelastic stress analysis of splinted and unitary implant-supported prostheses. *Appl. Phys. B.* 2014;**117**:235-244.

Perelli, M., Abundo, R., Corrente, G., Saccone, C. Short (5 and 7 mm long) porous implants in the posterior atrophic maxilla: a 5-year report of a prospective single-cohort study. *Eur. J. Oral. Implantol.* 2012;**5**:265-272.

Pesqueira, A.A., Goiato, M.C., Filho, H.G., Monteiro, D.R., Santos, D.M., Haddad, M.F., *et al.* Use of stress analysis methods to evaluate the biomechanics of oral rehabilitation with implants. *J. Oral. Implantol.* 2014;**40**:217-228.

Puri, N., Pradhan, K.L., Chandna, A., Sehgal, V., Gupta, R., Biometric study of tooth size in normal, crowded, and spaced permanent dentitions. *Am J Orthod Dentofacial Orthop.* 2007;**132**:279.e7-14.

Santiago Junior, J.F., Verri, F.R., Almeida, D.A., de Souza Batista, V.E., Lemos, C.A., Pellizzer, E.P.. Finite element analysis on influence of implant surface treatments, connection and bone types. *Mater. Sci. Eng. C. Mater. Biol. Appl.* 2016;**63**:292-300.

Pirmoradian M, Naeeni HA, Firouzbakht M, Toghraie D, Khabaz MK, Darabi R. Finite element analysis and experimental evaluation on stress distribution and sensitivity of dental implants to assess optimum length and thread pitch. *Comput Methods Programs Biomed.* 2019;**187**:105258.

Sertgöz, A. Finite element analysis study of the effect of superstructure material on stress distribution in an implant-supported fixed prosthesis. *Int. J. Prosthodont.* 1997;**10**:19-27.

Sevimay, M., Turhan, F., Kiliçarslan, M.A., Eskitascioglu, G. Three-dimensional finite element analysis of the effect of different bone quality on stress distribution in an implant-supported crown. *J. Prosthet. Dent. 2005;* **93**:227-234.

Solnit, G.S., Schneider, R.L. An alternative to splinting multiple implants: use of the ITI system. *J. Prosthodont.* 1998;**7**:114-119.

Sütpideler, M., Eckert, S.E., Zobitz, M., An, K.N. Finite element analysis of effect of prosthesis height, angle of force application, and implant offset on supporting bone. *Int. J. Oral. Maxillofac. Implants.* 2004;**19**:819-825.

Torcato, L.B., Pellizzer, E.P., Verri, F.R., Falcón-Antenucci, R.M., Batista, V.E., Lopes, L.F. Effect of the parafunctional occlusal loading and crown height on stress distribution. *Braz. Dent. J.* 2014;**25**:554-560.

Vázquez Álvarez, R., Pérez Sayáns, M., Gayoso Diz, P., García García, A. Factors affecting peri-implant bone loss: a post-five-year retrospective study. *Clin. Oral Implants Res.* 2015;**26**:1006-1014.

Verri, F.R., Batista, V.E., Santiago, J.F. Jr., Almeida, D.A., Pellizzer, E.P. Effect of crown-to-implant ratio on peri-implant stress: a finite element analysis. *Mater. Sci. Eng. C. Mater. Biol. Appl.* 2014;**45**:234-240.

Verri, F.R., Cruz, R.S., de Souza Batista, V.E., Almeida, D.A., Verri, A.C., Lemos, C.A., Santiago Júnior, J.F., Pellizzer, E.P. Can the modeling for simplification of a dental implant surface affect the accuracy of 3D finite element analysis? *Comput. Methods Biomech. Biomed. Engin.* 2016;**19**:1665-1672.

Verri, F.R., Santiago, J.F. Jr., Almeida, D.A., de Souza Batista, V.E., Araujo Lemos, C.A., Mello, C.C., Pellizzer, E.P. Biomechanical Three-Dimensional Finite Element Analysis of Single Implant-Supported Prostheses in the Anterior Maxilla, with Different Surgical Techniques and Implant Types. *Int. J. Oral Maxillofac. Implants.* 2017;**32**:e191-e198.

Weinberg, L.A., Kruger, B. An evaluation of torque (moment) on implant/prosthesis with staggered buccal and lingual offset. *Int. J. Periodontics Restorative Dent.* 1996;**1:** 252-265.